JOURNAL OF VIROLOGY, May 2005, p. 6180–6193 Vol. 79, No. 10
0022-538X/05/$08.00+0 doi:10.1128/JVI.79.10.6180–6193.2005
Copyright © 2005, American Society for Microbiology. All Rights Reserved.

Comparative Host Gene Transcription by Microarray Analysis Early after Infection of the Huh7 Cell Line by Severe Acute Respiratory Syndrome Coronavirus and Human Coronavirus 229E

Bone S. F. Tang,[1] Kwok-hung Chan,[1] Vincent C. C. Cheng,[1] Patrick C. Y. Woo,[1] Susanna K. P. Lau,[1] Clarence C. K. Lam,[2] Tsun-leung Chan,[3] Alan K. L. Wu,[1] Ivan F. N. Hung,[1] Suet-yi Leung,[3] and Kwok-yung Yuen[1]*

Department of Microbiology, Centre of Infection and Immunology, State Key Laboratory of Emerging Infectious Diseases, The University of Hong Kong,[1] and Division of Haematology[2] and Division of Anatomical Pathology,[3] Department of Pathology, The University of Hong Kong, Hong Kong

Received 21 October 2004/Accepted 11 January 2005

The pathogenesis of severe acute respiratory syndrome-associated coronavirus (SARS-CoV) at the cellular level is unclear. No human cell line was previously known to be susceptible to both SARS-CoV and other human coronaviruses. Huh7 cells were found to be susceptible to both SARS-CoV, associated with SARS, and human coronavirus 229E (HCoV-229E), usually associated with the common cold. Highly lytic and productive rates of infections within 48 h of inoculation were reproducible with both viruses. The early transcriptional profiles of host cell response to both types of infection at 2 and 4 h postinoculation were determined by using the Affymetrix HG-U133A microarray (about 22,000 genes). Much more perturbation of cellular gene transcription was observed after infection by SARS-CoV than after infection by HCoV-229E. Besides the upregulation of genes associated with apoptosis, which was exactly opposite to the previously reported effect of SARS-CoV in a colonic carcinoma cell line, genes related to inflammation, stress response, and procoagulation were also upregulated. These findings were confirmed by semiquantitative reverse transcription-PCR, reverse transcription-quantitative PCR for mRNA of genes, and immunoassays for some encoded proteins. These transcriptomal changes are compatible with the histological changes of pulmonary vasculitis and microvascular thrombosis in addition to the diffuse alveolar damage involving the pneumocytes.

Severe acute respiratory syndrome (SARS)-associated coronavirus (SARS-CoV) is the etiological agent of SARS (26, 39). The disease is associated with significant mortality and morbidity (38). Such aggressive clinical behavior is very different from that of other known human coronaviruses, such as the group 1 coronaviruses 229E and NL63 or the group 2 coronavirus OC43. Although these viruses are generally associated with mild upper respiratory tract infection such as the common cold (47–49), these human coronaviruses can also cause pneumonia when the very young, elderly, or immunosuppressed hosts are affected (14, 15, 40). Animal models of SARS were established by infecting cynomolgus monkeys, ferrets, domestic cats, or mice (16, 27, 31, 33, 55), but there are questions about their reproducibility of the pathology mimicking human disease. Although the cellular receptors for attachment of SARS-CoV were found to be ACE2 (30) and, recently, L-SIGN (23), pathogenesis at the cellular level is largely unknown.

SARS-CoV is an enveloped, positive-sense, single-stranded RNA virus which can grow in embryonal monkey cell lines, including Vero E6 and fetal rhesus monkey kidney (FRhk-4) cells (26, 39). It can be subcultured onto other Vero cells and colonic carcinoma cell lines such as Caco-2 or LoVo (3, 10). Unlike other human coronaviruses, SARS-CoV proliferates rapidly and causes obvious cytopathic effects in Vero E6 cells within 48 h of inoculation (35). There are no other human cell lines known to be susceptible to infection by both SARS-CoV and other human coronaviruses. Recently there have been reports of a human hepatoma cell line, Huh7, which can be infected by pseudotyped lentiviral particles carrying the spike protein of SARS-CoV and wild-type replicative SARS-CoV (6, 20, 45). We report in this study the susceptibility of the cell line Huh7 to infection by both SARS-CoV and human coronavirus 229E (HCoV-229E). A comparative gene transcriptional profile at an early stage of infection of Huh7 cells by these two viruses was performed to elucidate their difference and its importance in the pathogenesis of disease.

* Corresponding author. Mailing address: Department of Microbiology, State Key Laboratory of Emerging Infectious Diseases, Center of Infection and Immunology, Queen Mary Hospital, The University of Hong Kong, Hong Kong Special Administrative Region, China. Phone: 852-2855-4892. Fax: 852-2855-1241. E-mail: kyyuen@hkucc.hku.hk.

MATERIALS AND METHODS

Cell lines and virus. The human hepatoma cell line Huh7 (courtesy of David Ho, Aaron Diamond AIDS Research Center) was used throughout this study. The cells were incubated at 37°C in minimal essential medium supplemented with 10% fetal calf serum and 100 IU/ml of penicillin and 100 μg/ml of streptomycin. Our prototype virus (SARS-CoV HKU-39849) was isolated from the lung tissue biopsy of the brother-in-law of the index patient who traveled from Guangzhou and started a superspreading event in the Hong Kong Special Administrative Region leading to the pandemic (37). The HCoV-229E strain (ATCC VR-740) was used in this study. The SARS-CoV and HCoV-229E strains used in our experiments had undergone three passages in the FRhk-4 cell and MRC-5 cell lines, respectively, and were stored at −70°C. Viral titers were determined as median tissue culture infective dose ($TCID_{50}$) per ml in confluent Huh7 cells in 96-well microtiter plates, which standardized the viral inoculum and measured the relative susceptibility of the Huh7 cell line to these two viruses. The relative susceptibilities of the Vero 1008, Vero 76, Vero, and Huh7 cell lines

Downloaded from http://jvi.asm.org/ on March 10, 2015 by guest

to SARS-CoV and HCoV-229E were also tested by $TCID_{50}$. One hundred $TCID_{50}$ was confirmed by plaque assays to be equivalent to 85 PFU. All work with infectious virus was performed inside a type II biosafety cabinet in a biosafety containment level III facility, and the personnel wore powered air-purifying respirators (HEPA Airmate; 3 M, Saint Paul, Minn.).

Monitoring of virus-induced cytopathic effect, antigen detection, and semiquantitative and quantitative RT-PCR. Huh7 cells and culture supernatants infected with either SARS-CoV or HCoV-229E at a multiplicity of infection of 100 $TCID_{50}$ per cell were collected at 2, 4, 12, and 24 h postinfection. A washing step was performed 1 h postinoculation. The percentages of cells developing cytopathic effects were counted by inverted light microscopy at 24 and 48 h. The rate of viral replication was measured by reverse transcription-quantitative PCR (RT-qPCR) on the culture filtrate. The amount of coronavirus antigen expression in infected cells was measured by indirect immunofluorescence with convalescent-phase sera of patients with SARS-CoV or HCoV-229E infection, as reported previously (2, 8). Briefly, harvested cells were prepared and fixed in ice-cold acetone for 10 min. Convalescent-phase serum at a dilution of 1 in 100 was used to react with the infected cells harvested at various time points. After 30 min incubation, the cells were washed twice in phosphate-buffered saline for 5 min each, and then goat anti-human fluorescein isothiocyanate conjugate (INOVA Diagnostics, Inc., San Diego, CA) was added and the cells were further incubated for 30 min at 37°C. The cells were washed again as described above, and the percentage of positive cells was manually estimated under UV microscopy.

Reverse transcription-PCR (RT-PCR) for SARS-CoV and HCoV-229E was done directly on culture filtrate according to our previous protocol (2). Briefly, total RNA extracted from culture filtrate with the QIAamp virus RNA minikit (Qiagen) as instructed by the manufacturer was reverse transcribed with random hexamers. cDNA was amplified with SARS-CoV primers (forward, 5′-TACAC ACCTCAGCGTTG-3′; reverse, 5′-CACGAACGTGACGAAT-3′) and HCoV-229E primers (forward, 5′-GGTACTCCTAAGCCTTCTTCG-3′; reverse, 5′-G ACTATCAAACAGCATAGCAGC-3′). Using real-time RT-qPCR assays, cDNA was amplified in SYBR Green I fluorescence reactions (Roche, Mannheim, Germany). For the RT-qPCR of SARS-CoV, a 20-μl reaction mixtures containing 2 μl cDNA, 3.5 mmol/liter magnesium chloride, and 0.25 μmol/liter of the same forward and reverse primers as in the reaction mixtures were thermal cycled with a Light Cycler (Roche) (95°C for 10 min, followed by 50 cycles of 95°C for 10 s, 57°C for 5 s, and 72°C for 9 s with ramp rates of 20°C/s). For the RT-qPCR of HCoV-229E, the conditions were similar to those described above except that 45 cycles of 95°C for 10 s, 65°C for 3 s, and 72°C for 12 s were used. Plasmids with the target sequences were used to generate the standard curve. At the end of the assay, the PCR products of SARS-CoV and HCoV-229E (182 bp and 295 bp, respectively) were subjected to a melting curve analysis (65 to 95°C, 0.1°C/s) to determine the specificity of the assay. All assays were performed in replicates.

Microarray analysis. Human genome-wide gene expression was examined with the GeneChip system HG-U133A microarray (Affymetrix Inc., Santa Clara, CA), which is composed of more than 22,000 oligonucleotide probe sets interrogating approximately 18,400 unique transcripts, including 14,500 well-characterized human genes. Quality control, GeneChip hybridization, and data acquisition and analysis were performed at the Genome Research Centre, The University of Hong Kong, according to the standard protocols available from Affymetrix. In brief, total RNAs of the infected or uninfected cell lines at different time points were extracted using the RNeasy minikit (Qiagen, Valencia, CA). Double-stranded cDNA was synthesized from 10 μg of total RNA with the GeneChipT7-Oligo (dT) Promoter Primer Kit (Affymetrix, Inc.) and the SuperScript Choice System (Invitrogen). Biotin-labeled cRNA was then synthesized by in vitro transcription using the BioArray High Yield RNA Transcript Labeling Kit (Affymetrix, Inc). After fragmentation, 15 μg of labeled cRNA was hybridized to the oligonucleotide microarray. The chips were washed and stained using the GeneChip Fluidics Station 400 (Affymetrix) and then scanned with the GeneChip Scanner 3000 (Affymetrix). Data analysis was performed using the Microarray Suite Expression Analysis software (version 5.1; Affymetrix). For comparison across different arrays, the data for each array were normalized by a global scaling strategy, using a scaling target intensity of 500. By using the Affymetrix-defined comparison mathematical algorithms, a fold change in expression between each of the infected samples in comparison to the uninfected mock control was calculated, $\log_2$ transformed, and further classified as not changed, increased (signal log ratio change P value of <0.005), decreased (signal log ratio change P value of >0.995), or marginally increased or decreased. To classify a gene as significantly upregulated or downregulated after infection at a specific time point, two additional criteria were used: (i) the fold change must be greater than or equal to 2 (signal log ratio of ≥ 1 if upregulated or ≤ 1 if downregulated) to be classified as increased or decreased, and (ii) genes that were classified as upregulated must be flagged as present in the infected samples, while genes that were classified as downregulated must be flagged as present in the uninfected control sample. All gene chip procedures were performed in replicates.

Gene expression analysis by semiquantitative PCR, RT-qPCR, and immunoassays. Genes with significant transcriptional changes known to be associated with biological significance were selected for further analysis by semiquantitative PCR, RT-qPCR, and immunoassays. RT-qPCR was performed according to our previous protocol (56). The extracted RNA was pretreated with DNase. Primers which specifically amplified nine genes related to apoptosis, inflammation, and coagulation were designed (Table 1). First-strand cDNA was synthesized from the total RNA by reverse transcription with random hexamers. Semiqualitative comparison was performed using simple gel electrophoresis and ethidium bromide staining (10). Quantitative PCR was performed using the SYBR Green I fluorescence reactions in a Light Cycler as described above. Detailed PCR conditions are available upon request. Serial dilutions of a reference cDNA derived from the SARS-CoV-infected sample were used to generate the standard curve. Melting curve analysis was performed for each primer pair at the end of the reaction to confirm the specificity of the assay. The housekeeping porphobilinogen deaminase gene was used for standardization of the initial RNA content of a sample. Experiments were performed in duplicate, and the result for an individual sample was expressed as the mean expression level of a specific gene/porphobilinogen deaminase gene relative to the reference cDNA. The relative expression between each infected sample and the uninfected control was then calculated and expressed as fold change.

Three sets of immunoassays (human interleukin-8 [IL-8] from BD Biosciences and PAI1 [serpine 1] and TFPI2 from Diagnostica Stago) were performed according to our previous protocols (5, 28) and the manufacturers' instructions. Briefly, for IL-8 assay, 100 μl culture supernatant or standard was added to IL-8 monoclonal antibody-coated wells and incubated for 2 h at room temperature. After washing five times, 100 μl a biotinylated anti-human IL-8 monoclonal antibody was added to each well. After five washings, 100 μl of tetramethyl benzidine substrate was added, followed by incubation for 30 min at room temperature. The reaction was stopped by adding 50 μl stop solution. The absorbance was read at 450 nm within 30 min. The experimental conditions and procedure were similar for the immunoassays for PAI1 and TFP1. All experiments were done in replicates to ensure accuracy and reproducibility.

Statistical analysis. The fold change of the target gene expressions and the difference in the concentrations of expressed proteins between SARS-CoV and HCoV-229E at different postinoculation time points were compared by Student's t test. A P value of <0.05 was considered significant. A statistical package (SPSS 10.0; SPSS Hong Kong, Hong Kong) was used for all analyses.

RESULTS

Susceptibility of the Huh7 cell line to SARS-CoV and HCoV-229E. With a multiplicity of infection of 100, a cytopathic effect was visible in Huh7 cells at 24 and progressed to about 50% cell death at 48 h with both viruses. SARS-CoV but not HCoV-229E grew well in the Vero cell line. The viruses produced comparable $TCID_{50}$ of around 10^7 per ml in the culture supernatant of Huh7 cells at 48 h (Table 2). In terms of viral load, a 1-log-unit increase of viral genome copy was noted at 12 h postinoculation with both viruses, which was followed by a peak at 24 h (Table 3). Antigen expression could be observed by indirect immunofluorescence in over 50% of the cells at 24 h postinoculation for both viruses.

Effects on gene expression of host cells determined by microarray. Two hundred twenty-four genes were significantly altered within 4 h postinoculation in the transcriptomal expression analysis. Only 21 genes were perturbed by HCoV-229E per se, whereas 164 genes were altered by SARS-CoV infection only, and the remaining 39 genes were altered by both coronaviruses. Out of the 164 genes with altered expression in SARS-CoV, 38 were upregulated and only one was downregulated at both 2 and 4 h postinoculation. Forty-three were upregulated and 16 were downregulated at 2 h postinoculation.

Downloaded from http://jvi.asm.org/ on March 10, 2015 by guest

TABLE 1. Primers used for checking the expression of nine selected genes and a house keeping gene by semiquantitative RT- PCR and RT-qPCR

Gene product	Primer	Sequence (5′ to 3′)	Length (bp)	PCR product size (bp)
Tissue factor pathway inhibitor 2	TFPI2-F	CACCTATACTGGCTGTGGAGG	21	236
	TFPI2-R	CCTCATGCTGTCATATTATTCTTC	24	
Plasminogen activator inhibitor 1 (serpine 1)	PAI1-F	CCGAGGAGATCATCATGGAC	20	259
	PAI1-R	GCCAAGGTCTTGGAGACAGA	20	
Thrombospondin 1	THBS1-F	ATCATGGCTGACTCAGGACC	20	229
	THBS1-R	GGAAGCCAAGGAGAAGTGAT	20	
Interleukin-8	IL8-F	TGGAAGAGAGCTCTGTCTGGA	21	215
	IL8-R	CCAGGAATCTTGTATTGCATCT	22	
Nuclear factor of kappa light polypeptide gene enhancer in B-cells 2	NFKB2-F	CCTGGCAGGTCTACTGGAGG	20	281
	NFKB2-R	AAATAGGTGGGGACGCTGT	19	
Jun B proto-oncogene	JUNB-F	CCAGCTCAAACAGAAGGTCATG	22	209
	JUNB-R	GGAGTCCAGTGTGGTTTGCG	20	
Pleckstrin homology-like domain, family A, member 1	PHLDA1-F	CTCTCATCCTCACTCGCACC	20	214
	PHLDA1-R	TTGATCCAAGTGAAGACAATAGAA	24	
Caspase recruitment domain family, member 10	CARD10-F	CACGTGGAGGTGACTGAGAA	20	274
	CARD10-R	CTCAGGCCTCACTGCTGCT	19	
BCL2-associated X protein	BAX-F	GATGATTGCCGCCGTGGACA	20	175
	BAX-R	GATGGTTCTGATCAGTTCCGG	21	
Porphobilinogen deaminase	PBGD-F	AAGATGAGAGTGATTCGCGTG	21	226
	PBGD-R	GGTCCACTTCATTCTTCTCCAG	22	

Forty-nine were upregulated and 17 were downregulated at 4 h postinoculation. In contrast, for HCoV-229E infection, only one gene was upregulated and no gene was downregulated at both 2 and 4 h postinoculation. No gene was upregulated and two were downregulated at 2 h postinoculation. Fourteen genes were upregulated and four were downregulated at 4 h postinoculation. When multiple transcripts of the same gene were eliminated and analyzed, genes related to apoptosis (n = 23), inflammatory or immune response (n = 34), and coagulation (n = 5) were identified, in addition to the expected genes related to the stress response and metabolism and other unknown genes (Table 4). Of the 23 apoptotic genes affected, 13 of them are proapoptotic and 11 of them are upregulated in SARS-CoV infection, compared with only 3 in HCoV-229E infection (Table 5). For inflammation and immune response, 32 genes are upregulated in SARS-CoV, compared with only 3 in HCoV-229E. These include the genes for NFKB1A; NFKB2; IL-8; transforming growth factor β2; chemokines CXCL1, -2, -3, -5, -6, and -10; ICAM1; and tumor necrosis factor alpha-induced proteins. Quite unexpectedly, genes of the procoagulation pathway were also affected by SARS-CoV infection, with upregulation of PLSCR1 (phospholipid scramblase 1), EGR1 (early growth response 1 gene), PAI1/SERPINE1 (plasminogen activator inhibitor 1), and THBS1 (thrombospondin 1). In terms of stress response, seven genes were upregulated in SARS-CoV infection, compared with only one in HCoV-229E infection. Overall there were far more changes in expression of genes related to the cell cycle, transcription, and metabolism and those with miscellaneous and unknown functions in SARS-CoV infection. When the Pathway Assist software (Ariadne Genomics Inc.) was used for linking the altered genes in cellular pathways for SARS-CoV, there were clear clusterings of altered genes related to apoptosis, inflammation, and coagulation (Fig. 1).

TABLE 2. Viral load of SARS-CoV and HCoV-229E in different cell lines 48 h postinoculation

Cell line	Log_{10} $TCID_{50}$/ml	
	SARS Co-V	HCoV-229E
Vero 1008	6.5	ND[a]
Vero 76	8.33	ND
Vero	6.5	ND
Huh7	7.0	6.5

[a] ND, not detectable.

TABLE 3. Number of viral genome copies of SARS-CoV and HCoV-229E at different postinoculation time points in the Huh7 cell line

h postinoculation	Copies/ml	
	SARS-CoV	HCoV-229E
2	2.2×10^7	3.8×10^7
4	1.5×10^7	3.3×10^7
12	3.6×10^8	7.8×10^8
24	1.2×10^9	3.4×10^{10}

Downloaded from http://jvi.asm.org/ on March 10, 2015 by guest

TABLE 4. Numbers of genes with significant change of expression in different categories and subcategories

Category and subcategory	No. of genes			
	Total	SARS-CoV	HCoV-229E	Both SARS-CoV and HCoV-229E
Apoptosis	23			
Antiapoptosis	3	3	0	0
Proapoptosis	12	7	2	3
DNA repair	5	2	2	1
Other	3	2	1	0
Inflammation	34			
Antiinflammatory	2	2	0	0
Proinflammatory	24	21	0	3
Immunomodulatory	2	1	1	0
Other	6	5	1	0
Coagulation	5			
Anticoagulants	1	0	0	1
Procoagulants	4	4	0	0
Metabolism	35			
Amino acid	4	2	1	1
Carbohydrate	7	6	0	1
Lipid	5	5	0	0
Transporter	10	6	1	3
Other	9	7	2	0
Signal Transduction	18	15	1	2
Transcription	37	25	3	9
Cell Cycle	17	12	3	2
Cell growth and differentiation	7	6	0	1
Stress response	7	6	0	1
Miscellaneous	16	11	1	4
Unknown	25	16	2	7
Total	224	164	21	39

Confirmation of cellular gene and protein expression by semiquantitative PCR, RT-qPCR, and immunoassays. Since previous studies have documented the alterations of the apoptotic and inflammatory pathways in relation to SARS-CoV infection, only key genes related to inflammation and apoptosis were chosen to confirm the results of microarray analysis by semiquantitative RT-PCR and RT-qPCR. For the coagulation pathway, both procoagulation and anticoagulation genes were chosen. A similar trend of upregulation of gene expression was found by RT-qPCR, with SARS-CoV showing a 1.4- to 10.8-fold increase compared with HCoV-229E for coagulation (TFPI2, PAI1, and THBS1), inflammation (IL-8 and NFKB2), transcription (JUNB), and apoptotic (PHLDA1, CARD10, and BAX) pathways (Fig. 2 and 3). IL-8 was increased in both SARS-CoV and HCoV-229E infection, but the increase was much higher in the case of SARS-CoV. The enzyme immunoassay showed that SARS-CoV induced higher concentrations of PAI1 and IL-8 than HCoV-229E at 2, 4, 12, and 24 h postinoculation. Both SARS-CoV and HCoV-229E induced similar TFPI2 expression at 4, 12, and 24 h postinoculation, but at 2 h postinoculation SARS-CoV induced a lower concentration of this predominately anticoagulation protein (Fig. 4).

DISCUSSION

Of the four coronaviruses known to infect human, HCoV-229E, HCoV-OC43, and NL63 are generally associated with mild upper respiratory tract infection such as the common cold in immunocompetent hosts (47–49). In contrast, SARS-CoV causes respiratory failure in over 60% of affected persons, with a mortality rate of 15% (37, 38). Besides pneumonia, SARS is also clinically manifested as watery diarrhea without enterocolitis (48.6%) (8), hepatitis without liver failure (49.4%) (22), lymphopenia (75%) (37), impaired coagulation (63%) (51), and occasionally pulmonary vasculitis and thrombosis in the lungs of those who died (36, 13). Much is already known about many aspects of SARS, including the virology (18, 26, 39, 53), genomics (32), diagnostics (5, 28, 43, 52, 54), clinical features and progression in relation to viral load (22, 37), treatment (7, 9, 46), infection control (44), and immunization (55). However little is known about the pathogenesis at the cellular level, despite the identification of ACE2 and L-SIGN as the receptors for binding of SARS-CoV to host cells (30, 23).

One important limitation to studies at the cellular level is the absence of a relevant cell line which can be lytically infected by SARS-CoV. Initially, only embryonal monkey kidney cell lines such as Vero or FRhk-4 and their derivatives could be readily infected. Subsequent investigation showed that human colon adenocarcinoma cell lines Caco-2, CL-14, and LoVo could also be infected (3, 10). However, inflammation or cell death is not manifested on endoscopic examination of the intestines of SARS patients (29). Examination of intestinal tissue biopsy by electron microscopy revealed abundant intracellular viral particles, and there was negligible inflammatory cells or cellular apoptosis on light microscopy (29). In fact, a high $TCID_{50}$ in the culture supernatant of persistently infected LoVo cells can be achieved without any cytopathic effects (3). Recently a gene expression analysis showed that SARS-CoV upregulated antiapoptotic genes and several CXC chemokines while downregulating proapoptotic genes, IL-18, and macrophage migration inhibitory factor (10) at 24 h postinoculation of Caco-2 cell lines. These patterns of gene expression appeared to explain the severe watery diarrhea without clinical or endoscopic signs of necrosis or inflammation in SARS patients (29). However, no data on early gene expression before the onset of cytolysis were reported. Similarly, no comparative study of the host cell transcriptional profile and those for other, less virulent coronaviruses was ever reported.

No pneumocyte cell line has yet been found to support lytic or nonlytic infection by SARS-CoV. However, the human hepatoma cell line Huh7 was found to be susceptible to SARS-CoV. This is not completely unexpected, because the mouse hepatitis virus, a group 2 coronavirus, is known to infect Huh7 cells (25). In this study HCoV-229E was found to produce good lytic infection within 48 h postinoculation. A high multiplicity of infection of 100 $TCID_{50}$s per cell was used to ensure the reproducibility of gene expression, as previously reported (41). Since the expression of a high number of genes was expected to change significantly when virus-induced cytopathology was impending for a rapidly lytic viral infection, we

Downloaded from http://jvi.asm.org/ on March 10, 2015 by guest

TABLE 5. Signal log ratios (log_2 scale) of the genes that are significantly altered after SARS-CoV or HCoV-229E infection

Category and subcategory	Gene: Affymetrix identification no.	Gene: Designation	Description	Signal log ratio (log_2 scale)[a] after infection with: HCoV-229E 2 h	HCoV-229E 4 h	SARS-CoV 2 h	SARS-CoV 4 h
Apoptosis							
Antiapoptosis	200797_s_at	MCL1	Myeloid cell leukemia sequence 1 (BCL2 related)	0.2	0	1	0.3
	210538_s_at	BIRC3	Baculoviral IAP repeat containing 3	0.2	0.6	**2.1**	1.4
	201631_s_at	IER3	Immediate-early response 3	0.3	−0.2	1.7	1.3
Apoptosis	204285_s_at	PMAIP1[b]	Phorbol-12-myristate-13-acetate-induced protein 1	0.5	−0.2	1.6	0.6
	204908_s_at	BCL3[b]	B-cell CLL/lymphoma 3	0.1	0.1	1.9	1.1
	207181_s_at	CASP7	Caspase 7, apoptosis-related cysteine protease	−0.2	0.4	0.1	1.2
	208478_s_at	BAX	BCL2-associated X protein	0.5	0.6	0.4	1.1
	208536_s_at	BCL2L11	BCL2-like 11 (apoptosis facilitator)	−1.3	0.3	0.1	1.2
	209305_s_at	GADD45B[b]	Growth arrest and DNA-damage-inducible, beta	0.1	−0.2	1.4	0.8
	210025_s_at	CARD10[b]	Caspase recruitment domain family, member 10	1	−0.4	1.9	**2.7**
	211085_s_at	STK4	Serine/threonine kinase 4	0.4	1.3	0.2	0.6
	211695_x_at	MUC1	Mucin 1, transmembrane	−0.2	−1.3	−0.1	−0.8
	218368_s_at	TNFRSF12A	Tumor necrosis factor receptor superfamily, member 12A	0.5	0	1	0.6
	218880_at	FOSL2	FOS-like antigen 2	1.8	−0.4	**3.3**	1.5
	217997_at[b]	PHLDA1	Pleckstrin homology-like domain, family A, member 1	0.5	0.1	**2.9**	1.6
DNA repair	205022_s_at	CHES1	Checkpoint suppressor 1	0	−0.2	0.2	−1
	205072_s_at	XRCC4	X-ray repair complementing defective repair in Chinese hamster cells 4	−1.1	−0.2	−1.3	−0.3
	208386_x_at	DMC1	DMC1 dosage suppressor of mck1 homolog, meiosis-specific homologous recombination	−0.1	1.2	0.4	0.2
	209579_s_at	MBD4	Methyl-CpG binding domain protein 4	0.1	0.6	0.2	1
	219317_at	POLI	Polymerase (DNA directed) iota	0	1.1	−0.6	0.5
Other	204178_s_at	RBM14	RNA binding motif protein 14	−0.3	0.5	−0.3	1
	209803_s_at	PHLDA2	Pleckstrin homology-like domain, family A, member 2	0.1	0.1	0.4	1
	215338_s_at	NKTR	Natural killer-tumor recognition sequence	0.8	1	0.3	0.2
Inflammation							
Anti-inflammatory	201502_s_at	NFKBIA/IKBA	Nuclear factor of kappa light polypeptide gene enhancer in B-cells inhibitor, alpha/I-kappa B alpha	0.2	−0.1	1.4	0.5
	221577_x_at	PLAB	Prostate differentiation factor	0.6	−0.2	1.8	0.5
Proinflammatory	202510_s_at	TNFAIP2	Tumor necrosis factor alpha-induced protein 2	−0.3	−0.3	1.2	1.2
	202625_at	LYN[b]	v-yes-1 Yamaguchi sarcoma viral related oncogene homology/oncogene LYN	0.1	−0.1	−0.2	1.2
	202637_s_at	ICAM1[b]	Intercellular adhesion molecule 1 (CD54), human rhinovirus receptor	0.2	−0.3	**2.5**	1.8
	202644_s_at	TNFAIP3[b]	Tumor necrosis factor alpha-induced protein 3	0.2	−0.1	**2.1**	1
	203313_s_at	TGIF	TGFB-induced factor (TALE family homeobox)	0.5	0.3	1	1
	203964_at	NMI	N-myc (and STAT) interactor (transcription from Pol II promoter, inflammatory response, JAK-STAT cascade)	0	0.2	0.2	1
	204470_at	CXCL1	Chemokine (C-X-C motif) ligand 1 (melanoma growth-stimulating activity, alpha)	0.8	−0.2	**3.1**	0.9
	205114_s_at	CCL3/MIP1A	Chemokine (C-C motif) ligand 3/macrophage inflammatory protein 1-alpha	0.5	0.4	1.4	1
	205476_at	CCL20/MIP3A	Chemokine (C-C motif) ligand 20/macrophage inflammatory protein 3-alpha	0.4	−0.2	1.2	0.8
	205844_at	VNN1	Vanin 1	−0.6	0.3	0.1	1.2
	205922_at	VNN2	Vanin 2	0.7	−0.2	0.8	1
	206336_at	CXCL6	Chemokine (C-X-C motif) ligand 6 (granulocyte chemotactic protein 2)	0.2	0.4	0.5	1.3
	207850_at	CXCL3/MIP2B	Chemokine (C-X-C motif) ligand 3/macrophage inflammatory protein 2-beta	0.2	1.6	**5.2**	**3.5**
	208991_at	STAT3	Signal transducer and activator of transcription 3 (acute-phase response factor)	0	−0.5	1	0.4

Continued on facing page

Downloaded from http://jvi.asm.org/ on March 10, 2015 by guest

TABLE 5—*Continued*

Category and subcategory	Gene		Description	Signal log ratio (log_2 scale)[a] after infection with:			
				HCoV-229E		SARS-CoV	
	Affymetrix identification no.	Designation		2 h	4 h	2 h	4 h
	209636_at	NFKB2[b]	Nuclear factor of kappa light polypeptide gene enhancer in B cells 2	−0.8	−1.4	**2.5**	**2.7**
	209774_x_at	CXCL2/MIP2A	Chemokine (C-X-C motif) ligand 2/macrophage inflammatory protein 2-alpha	1.1	0	**3**	1.6
	209909_s_at	TGFB2[b]	Transforming growth factor beta 2	0.1	0.2	0.9	**2.1**
	211000_s_at	IL-6ST[b]	Interleukin-6 signal transducer (gp130, oncostatin M receptor)	0.5	0.9	0	1.3
	211506_s_at	IL-8[b]	Interleukin-8	0.6	0.7	**3.3**	**2.1**
	212063_at	CD44	CD44 antigen (homing function and Indian blood group system)	0.1	−0.1	0.5	1.1
	212989_at	CXCL10	Chemokine (C-X-C motif) ligand 10 or Mob protein	0.2	0.6	0.9	1
	215101_s_at	CXCL5	Chemokine (C-X-C motif) ligand 5	−0.2	0.4	1.6	**2**
	217738_at	PBEF[b]	Pre-B-cell colony-enhancing factor	0	−0.1	1.5	1.3
	AFFX-HUMISGF3A/M97935_5_at	ISGF-3	Interferon-stimulated transcription factor 3	0.1	0.4	0.4	1.3
Immuno-modulatory	201667_at	GJA1/CX43	Gap junction protein, alpha 1/gap junction protein 43-KD/connexin 43/heart connexin	0	0.3	0.7	1.4
	220954_s_at	PILR, BETA	Paired immunoglobulin-like receptor beta	−0.2	1	−0.3	0.9
Other	202531_at	IRF1	Interferon regulatory factor 1	0.1	−0.6	1	0.1
	204622_x_at	NR4A2	Nuclear receptor subfamily 4, group A, member 2	0.3	−0.3	−1.6	−0.9
	204897_at	PTGER4	Prostaglandin E receptor 4 (subtype EP4)	0.2	0.2	1.2	1.1
	205220_at	Chemokine receptor HM74	Putative chemokine receptor	0.2	−0.1	1.7	1
	206785_s_at	KLRC2	Killer cell lectin-like receptor subfamily C, member 2	0.3	**2.2**	**3.8**	**5.2**
	220491_at	HAMP	Hepcidin antimicrobial peptide	0.4	−0.4	**2.1**	0.2
Coagulation							
Anticoagulants	209277_at	TFPI2[b]	Tissue factor pathway inhibitor 2	1	0.9	**2.1**	**3**
Procoagulants	202446_s_at	PLSCR1/MMTRA1B	Phospholipid scramblase 1	0	0.2	0.6	1.2
	201110_s_at	THBS1[b]	Thrombospondin 1	0.5	0.2	**2.3**	1.1
	201693_s_at	EGR1[b]	Early growth response 1	0.1	−0.9	1	−1.1
	202627_s_at	PAI1	Plasminogen activator inhibitor 1, serpine 1	−0.4	−0.6	1.3	1.8
Metabolism							
Amino acid	201739_at	SGK	Serum/glucocorticoid regulated kinase	0.2	−0.2	1	0.4
	206669_at	GAD1	Glutamate decarboxylase 1 (brain, 67 kDa)	0.1	**2.9**	**2.8**	**3**
	219795_at	SLC6A14	Solute carrier family 6 (neurotransmitter transporter), member 14	−0.1	0.4	1.1	**2**
	222018_at	NACA	Nascent-polypeptide-associated complex alpha polypeptide	0.3	1	−0.4	0.4
Carbohydrate	202464_s_at	PFKFB3	6-Phosphofructo-2-kinase/fructose-2,6-biphosphatase 3	0.1	0.3	1.1	1.1
	214850_at	SMA5	*H. sapiens* beta glucuronidase pseudogene	1	1.5	0.8	**2.1**
	215977_x_at	GK	Glycerol kinase	0	0.6	0.8	1
	218918_at	MAN1C1	Mannosidase, alpha, class 1C, member 1	−0.3	0.2	−0.8	−1
	218985_at	SLC2A8	Solute carrier family 2 (facilitated glucose transporter), member 8	−0.1	0.4	0.3	1
	219508_at	GCNT3	Glucosaminyl (*N*-acetyl) transferase 3, mucin type	0.2	0.1	1	1
	219797_at	MGAT4A	Mannosyl (alpha-1,3-)-glycoprotein beta-1,4-*N*-acetylglucosaminyltransferase, isoenzyme A	0.4	0.7	0.9	1.2

Continued on following page

Downloaded from http://jvi.asm.org/ on March 10, 2015 by guest

TABLE 5—*Continued*

Category and subcategory	Gene		Description	Signal log ratio (log_2 scale)[a] after infection with:			
	Affymetrix identification no.	Designation		HCoV-229E		SARS-CoV	
				2 h	4 h	2 h	4 h
Lipid	202067_s_at	LDLR[b]	Low-density lipoprotein receptor (familial hypercholesterolemia)	0.5	−0.3	1.5	−0.3
	204242_s_at	ACOX3	Acyl coenzyme A oxidase 3, pristanoyl	0.3	0	0.5	1.3
	205769_at	SLC27A2	Solute carrier family 27 (fatty acid transporter), member 2	0	−0.3	−0.6	−1.2
	205822_s_at	HMGCS1	3-Hydroxy-3-methylglutaryl coenzyme A synthase 1 (soluble)	0	0.8	0.7	1
	212226_s_at	PPAP2B[b]	Phosphatidic acid phosphatase type 2B	0	−0.3	1.2	−0.3
Transporters	202437_s_at	CYP1B1[b]	Cytochrome P450, family 1, subfamily B, polypeptide 1	0.6	1.5	**3**	**3.5**
	204685_s_at	ATP2B2	ATPase, Ca^{2+} transporting, plasma membrane 2	0	−0.3	0.1	−1
	205195_at	AP1S1[b]	Adaptor-related protein complex 1, sigma 1 subunit	1.7	1.7	1	**2.1**
	205749_at	CYP1A1	Cytochrome P450, family 1, subfamily A, polypeptide 1	−0.4	1.7	1.6	**2.5**
	207604_s_at	SLC4A7[b]	Solute carrier family 4, sodium bicarbonate cotransporter, member 7	0.3	0.6	0.7	1.4
	208914_at	GGA2	Golgi-associated, gamma adaptin ear-containing, ARF binding protein 2	−0.2	−0.5	−0.2	−1
	210357_s_at	SMOX	Spermine oxidase	0	−0.2	1.2	1.3
	211572_s_at	SLC23A1	Solute carrier family 23 (nucleobase transporters), member 1	0.3	0.1	0	1
	218703_at	SEC22L2	SEC22 vesicle trafficking protein-like 2	1	1.3	−0.5	0.9
	220786_s_at	SLC38A4	Solute carrier family 38, member 4	−0.2	0	−0.7	−1.1
Miscellaneous	201556_s_at	VAMP2	Vesicle-associated membrane protein 2 (synaptobrevin 2)	0	−1.8	−0.7	−0.8
	202238_s_at	NNMT[b]	Nicotinamide *N*-methyltransferase	0.4	0.5	1.9	**2.8**
	203798_s_at	VSNL1	Visinin-like 1	−0.1	−0.1	0	−1
	206293_at	SULT2A1	Sulfotransferase family, cytosolic, 2A, dehydroepiandrosterone preferring, member 1	−0.2	0	−0.3	−1
	208776_at	PSMD11	Proteasome (prosome, macropain) 26S subunit, non-ATPase, 11	0	−0.3	−0.2	−1
	210447_at	GLUD2	Glutamate dehydrogenase 2	−0.2	−0.1	−0.9	−1
	213926_s_at	HRB	HIV-1[c] Rev binding protein	0.2	0.4	0.3	1
	214837_at	ALB	Albumin	−0.2	1.2	−0.7	0.2
	216049_at	RHOBTB3	Rho-related BTB domain-containing 3	−0.5	−0.4	−1	−0.6
Signal transduction	201010_s_at	TXNIP	Thioredoxin-interacting protein	−0.5	−0.2	−1.6	−0.6
	201044_x_at	DUSP1[b]	Dual-specificity phosphatase 1	0.1	−0.4	**3.2**	**2.1**
	201295_s_at	WSB1	SOCS box-containing WD protein SWiP-1	0.2	1.6	−0.2	1.4
	201824_at	RNF14	Ring finger protein 14	−0.2	−0.1	−1.2	−0.3
	203879_at	PIK3CD	Phosphoinositide-3-kinase, catalytic, delta polypeptide	−0.2	−0.3	0.1	1.2
	205205_at	RELB	v-Rel reticuloendotheliosis viral oncogene homolog B, nuclear factor of kappa light polypeptide gene enhancer in B cells 3 (avian)	0.3	−0.5	1.4	0.8
	205239_at	AREG	Amphiregulin (schwannoma-derived growth factor)	0.4	0.8	1.5	0.7
	205868_s_at	PTPN11	Protein tyrosine phosphatase, non-receptor type 11 (Noonan syndrome 1)	0.6	1.6	0.6	0.8
	210056_at	RHO6	GTP binding protein	0.7	0.3	**3.8**	**2.6**
	211962_s_at	ZFP36L1	Zinc finger protein 36	0.2	0	1.1	0.7
	212099_at	ARHB	Ras homolog gene family, member B	0.2	−0.5	1.3	0.6
	212777_at	SOS1[b]	Son of sevenless homolog 1 (Drosophila)	0	0.8	0.6	1.2
	213848_at	DUSP7	Dual-specificity phosphatase 7	−0.3	0.1	−1	−0.2
	213880_at	GPR49	G protein-coupled receptor 49	0.2	0.5	−0.4	1.7
	218295_s_at	NUP50	Nucleoporin, 50 kDa	0.2	0.8	0.4	1
	219677_at	SSB1	SPRY domain-containing SOCS box protein SSB-1	0.4	0.2	1.4	0.6

Continued on facing page

Downloaded from http://jvi.asm.org/ on March 10, 2015 by guest

TABLE 5—*Continued*

Category and subcategory	Gene		Description	Signal log ratio (log_2 scale)[a] after infection with:			
	Affymetrix identification no.	Designation		HCoV-229E		SARS-CoV	
				2 h	4 h	2 h	4 h
	41660_at	CELSR1	Cadherin epidermal growth factor LAG seven-pass G-type receptor 1	0.7	0.6	0.4	1.1
	AFFX-HUMRGE/M10098_5_at	GPR34	G protein-coupled receptor 34	**−2.7**	**3**	0.9	**3.7**
Transcription	201169_s_at	BHLHB2[b]	Basic helix-loop-helix domain containing, class B, 2	0	0	1.3	1.8
	201473_at	JUNB	Jun B proto-oncogene	0.5	−0.3	**2.4**	**2.2**
	201510_at[b]	ELF3*	E74-like factor 3 (Ets domain transcription factor, epithelial specific)	0.5	0	1.9	1.3
	202601_s_at	HTATSF1/TATSF1	HIV TAT specific factor 1	0.7	1.4	0.9	1.1
	202672_s_at	ATF3	Activating transcription factor 3	0.6	−0.6	**2.2**	0.1
	202935_s_at	SOX9	SRY (sex determining region Y)-box 9 (campomelic dysplasia, autosomal sex reversal)	0.4	−0.3	1.1	−0.3
	203751_x_at	JUND[b]	Jun D proto-oncogene	0.5	−1.2	1.4	−0.4
	203973_s_at	CEBPD	CCAAT/enhancer binding protein (C/EBP), delta	0.6	−0.6	**2.3**	1.5
	204069_at	MEIS1	Meis1, myeloid ecotropic viral integration site 1 homolog (mouse)	−1.1	0.3	−0.7	0.1
	205187_at	SMAD5	Mothers against DPP homolog 5 (*Drosophila*) SMAD	0.9	1	1.3	1.4
	205398_s_at	SMAD3	SMAD, mothers against DPP homolog 3 (*Drosophila*)	0.4	0.1	1	1.1
	205443_at	SNAPC1	Small nuclear RNA activating complex, polypeptide 1	0.4	0.6	1	0.8
	205471_s_at	DACH1	Dachshund homolog (*Drosophila*) 1	0.4	−0.6	−0.1	−1
	205975_s_at	HOXD1	Homeo box D1	0	−0.3	1	0.7
	206036_s_at	REL	v-Rel reticuloendotheliosis viral oncogene homolog (avian)	0.4	0.2	1	0.1
	206175_x_at	ZNF222	Zinc finger protein 222	0.2	1	0.1	0.5
	207147_at	DLX2	Distal-less homeo box 2	0.7	−1.8	1.5	1.7
	207558_s_at	PITX2	Paired-like homeodomain transcription factor 2	−0.2	1.1	−1	−0.1
	208129_x_at	RUNX1	Runt-related transcription factor 1 (acute myeloid leukemia 1; am11 oncogene)	0.5	0.7	1	0.4
	209291_at	ID4	Inhibitor of DNA binding 4, dominant negative helix-loop-helix protein	0.2	−0.2	−0.6	−1
	209357_at[b]	CITED2[b]	Cbp/p300-interacting transactivator, with Glu/Asp-rich carboxy-terminal domain, 2	0.1	−0.1	−1.4	−0.2
	209505_at	NR2F1	Nuclear receptor subfamily 2, group F, member 1	−0.1	−0.2	−1	−0.3
	209757_s_at	MYCN	v-Myc myelocytomatosis viral related oncogene, neuroblastoma derived (avian)	0.2	−0.3	−1.1	−0.7
	212641_at	HIVEP2	HIV-2 1 enhancer-binding protein 2	0.3	−0.1	1.8	0.2
	213668_s_at	SOX4[b]	SRY (sex-determining region Y) box 4	0.5	0.7	1.8	1.3
	213844_at	HOXA5	Homeo box A5	−0.1	0.1	1.1	1
	213906_at	MYBL1	v-Myb myeloblastosis viral oncogene homolog (avian)-like 1	−0.5	0.4	−1	0.2
	214639_s_at	HOXA1	Homeo box A1	−1.1	−1.2	1.3	1.9
	215073_s_at	NR2F2[b]	Nuclear receptor subfamily 2, group F, member 2	0.1	0	−1.2	−0.5
	215720_s_at	NFYA	Nuclear transcription factor Y, alpha	0.4	1.6	0.8	1.4
	218559_s_at	MAFB	v-Maf musculoaponeurotic fibrosarcoma oncogene homolog B (avian)	−0.4	0	−1.4	−1.3
	220444_at	ZNF557	Zinc finger protein 557	**2.3**	**2.2**	0.9	**2.4**
	221773_at	ELK3	ETS domain protein	−0.3	0.1	−0.1	1
	221883_at	PKNOX1	PBX/knotted 1 homeobox 1	0.8	0.9	0.2	1.7
	36711_at	MAFF[b]	v-Maf musculoaponeurotic fibrosarcoma (avian) oncogene family	0.6	−1	1.9	0
	40837_at	TLE2	Transducin-like enhancer of split 2 [E(sp1) homolog, *Drosophila*]	−0.6	−1	−0.5	−0.5
	44783_s_at	HEY1	Hairy/enhancer-of-split related with YRPW motif 1	0	0.3	0.6	1.3

Continued on following page

Downloaded from http://jvi.asm.org/ on March 10, 2015 by guest

TABLE 5—*Continued*

Category and subcategory	Gene		Description	Signal log ratio (log_2 scale)[a] after infection with:			
	Affymetrix identification no.	Designation		HCoV-229E		SARS-CoV	
				2 h	4 h	2 h	4 h
Cell cycle	201055_s_at	HNRPA0	Heterogeneous nuclear ribonucleoprotein A0	0.1	0.6	0.5	1
	202150_s_at	NEDD9	Neural precursor cell expressed, developmentally downregulated 9	0	−0.8	1.1	0.8
	202768_at	FOSB	FBJ murine osteosarcoma viral oncogene homolog B	−0.3	−0.4	**3.8**	−0.1
	202769_at	CCNG2[b]	Cyclin G2	0.1	0	−0.2	1.5
	203120_at	TP53BP2	Tumor protein p53 binding protein, 2	0.3	0.2	1.1	0.4
	204137_at	TM7SF1	Transmembrane 7 superfamily member 1 (upregulated in kidney)	1.7	1.6	1.3	**2.7**
	204159_at	CDKN2C	Cyclin-dependent kinase inhibitor 2C (p18, inhibits CDK4)	−0.2	0.1	−1.3	−0.7
	205027_s_at	MAP3K8	Mitogen-activated protein kinase kinase kinase 8	−0.1	0.7	1.9	0.7
	205046_at	CENPE	Centromere protein E	0.1	1.1	−0.1	0.8
	205425_at	HIP1	Huntingtin-interacting protein 1	−0.1	−1	−0.7	−0.9
	207530_s_at	CDKN2B	Cyclin-dependent kinase inhibitor 2B (p15, inhibits CDK4)	0.4	**2.3**	**2.5**	**3.9**
	209680_s_at	KIFC1	Kinesin family member C1	0	0.4	−0.6	1
	210136_at	MBP	Myelin basic protein	0.4	0.5	1.1	0.9
	212000_at	SFRS14	Arginine/serine-rich 14 splicing factor	0.8	1.2	0.4	0.8
	212769_at	TLE3	Transducin-like enhancer of split 3 [E(sp1) homolog, *Drosophila*]	0	0.2	1.2	0.7
	221841_s_at	KLF4	Kruppel-like factor 4	0.4	−0.8	1.3	0
	222303_at	ETS2	v-Ets avian erythroblastosis virus E26 oncogene homolog 2	−0.2	0.5	1.2	0.8
Cell growth and differentiation	201329_s_at	ETS2[b]	v-Ets crythroblastosis virus E26 oncogene homolog 2 (avian)	0.3	0.1	**2**	1.3
	201341_at[b]	ENC1/PIG10/NRPB	Ectodermal-neural cortex (with BTB-like domain) p53-induced gene 10; nuclear restricted protein/brain	0	0.2	0.8	1.2
	207401_at	PROX1	Prospero-related homeobox 1	0.3	0.5	1.2	1.1
	210001_s_at	SOCS1	Suppressor of cytokine signaling 1	0.2	−0.5	1.1	0.4
	210587_at	INHBE	Inhibin, beta E	0.2	−0.1	0.9	1.1
	213004_at	ANGPTL2	Angiopoietin-like 2	−0.1	0.1	0.3	1
	216684_s_at	SS18[b]	Synovial sarcoma translocation, chromosome 18	0.9	1.5	1.3	1.7
Stress response	200664_s_at	DNAJB1	Heat shock 40-kDa protein 1	0.1	0.4	1	0.7
	202376_at	AACT/SERPINA3	Alpha-1 antichymotrpysin/serine (or cysteine) proteinase inhibitor, clade A (alpha-1 antiproteinase, antitrypsin), member 3	−0.4	−0.8	1.4	1.3
	202581_at	HSPA1B/HSP70-2	Heat shock 70-kDa protein 1B/heat shock protein, 70 kDa 2	−0.2	0.8	−0.2	1
	208607_s_at	SAA2	Serum amyloid A2	**2.7**	**2**	**3.5**	**3.7**
	209799_at	PRKAA1	Protein kinase, AMP activated, alpha 1 catalytic subunit	0	0.7	0.2	1.1
	215078_at	SOD2[b]	Superoxide dismutase 2, mitochondrial	0.4	0.4	3	1.7
	221477_s_at	SOD7	Superoxide dismutase 2, mitochondrial	0	0.1	1.1	1.3
Miscellaneous	202241_at	TR1B1	Tribbles homolog 1 (*Drosophila*)	−0.1	−0.6	1.1	0.3
	202458_at	SPUVE	Protease, serine, 23	0.1	0.2	0.4	1
	202760_s_at	AKAP2	A kinase (PRKA) anchor protein 2	0.6	0	1.1	0.1
	203234_at	UPP1	Uridine phosphorylase 1	−0.6	0.3	0.3	1.3
	205890_s_at	UBD	Ubiquitin D	0	−0.2	1.3	**2**
	206374_at	DUSP8	Dual-specificity phosphatase 8	0.6	−0.6	1.7	−0.7
	210159_s_at	TRIM31[b]	Tripartite motif-containing 31	**2.2**	1.1	**2.3**	**3**
	212027_at	RBM25	RNA binding motif protein 25	0.2	1.1	0.3	0.9
	212244_at	GRINL1A	Glutamate receptor, ionotropic, *N*-methyl D-aspartate-like 1A	−0.2	−0.1	−1	−0.2
	212905_at	CSTF2T	Cleavage stimulation factor, 3′ pre-RNA, subunit 2, 64 kDa, tau variant	−0.5	0	−1.1	0.1

Continued on facing page

Downloaded from http://jvi.asm.org/ on March 10, 2015 by guest

TABLE 5—*Continued*

Category and subcategory	Gene		Description	Signal log ratio (log_2 scale)[a] after infection with:			
	Affymetrix identification no.	Designation		HCoV-229E		SARS-CoV	
				2 h	4 h	2 h	4 h
	213006_at	KIAA0146	KIAA0146 protein	0.2	−0.6	1.8	1.1
	217475_s_at	LIMK2	LIM domain kinase 2	0.2	0.3	1	0.5
	218737_at	SBNO1	Sno, strawberry notch homolog 1	0.9	1	0.3	1
	218810_at	FLJ23231	Hypothetical protein FLJ23231	−1	**−3.5**	**2.7**	1.3
	220992_s_at	C1orf25	Chromosome 1 open reading frame 25	0.1	1.2	−0.1	1
	221258_s_at	DKFZP434G2226	Kinesin family member 18A	0	0.6	−0.9	1
Unknown functions	204447_at	ProSAPiP1	ProSAPiP1 protein	0.1	−0.8	0	−1.2
	204492_at	ARHGAP11A	KIAA0013 gene product	0.5	1	−0.2	0.5
	208154_at	LOC51336	Mesenchymal stem cell protein DSCD28	−0.7	−0.3	−0.1	−1.2
	212686_at	PPM1H	Protein phosphatase 1H (PP2C domain containing)	0	−0.4	−0.1	−1.1
	212845_at	SAMD4	Sterile alpha motif domain containing 4	0.1	−0.4	1	−0.5
	213069_at	HEG[b]	HEG homolog	0.3	−0.3	1.1	−0.2
	213256_at	MGC48332	Hypothetical protein MGC48332	0	0.2	0.4	1.1
	214077_x_at	MEIS3	Meis1, myeloid ecotropic viral integration site 1 homolog 3 (mouse)	0.5	0.4	0.3	1.2
	214862_x_at		MRNA; cDNA DKFZp564G1162	−0.1	−0.1	−1	−0.6
	215281_x_at	POGZ	Pogo transposable element with ZNF domain	0	1	0.1	−0.3
	216715_at			1.2	1.3	1	1.1
	217047_s_at	FAM13A1[b]	Family with sequence similarity 13, member A1	−0.3	0.6	−1	−0.1
	217300_at			−1	−0.2	−1	−0.4
	218031_s_at	C14orf116	Chromosome 14 open reading frame 116	0.1	−0.7	0.2	−1
	218541_s_at	C8orf4	Chromosome 8 open reading frame 4	0.4	0.1	1.3	0.9
	218816_at	LANO	LAP (leucine-rich repeats and PDZ) and no PDZ protein	0.1	0.3	0	1
	219010_at	FLJ10901	Hypothetical protein FLJ10901	−0.1	0.1	1	1.6
	219166_at	C14orf104	Chromosome 14 open reading frame 104	−0.4	0.3	−1.3	0.4
	219696_at	FLJ20054	Hypothetical protein FLJ20054	0.1	−0.1	−0.2	−1
	220041_at	SMP3	SMP3 mannosyltransferase	−0.4	−1.1	−0.5	−1
	220441_at	FLJ13236	Hypothetical protein FLJ13236	0	0.4	0.5	1.4
	220770_s_at	LOC63920	Transposon-derived Buster3 transposase-like	−0.6	1.3	−0.8	1
	222196_at	LOC286434	Hypothetical protein LOC286434	1.1	0.8	0.9	**2.2**
	AFFX-r2-Hs18SrRNA-M_x_at		Human 18S rRNA[b]	**−2.1**	1.7	0.7	**2.6**
	AFFX-r2-Hs28SrRNA-3_at		Human 28S rRNA[b]	−1.4	0.7	0.5	1.2

[a] Minus, decreased gene expression; no minus, increased gene expression; underlining, two-to fourfold-increased or decreased gene expression; boldface, >4-fold-increased or decreased gene expression.
[b] More than one probe set has a significant change in gene expression; only the most representative is shown.
[c] HIV-1, human immunodeficiency virus type 1.

tried to study the difference in the expression profile at the relatively early stages of the infection of 2 and 4 h postinoculation, as reported for herpes simplex virus type 1 (17). This time frame is biologically relevant because proliferation of the Golgi complex and related vesicles and swelling of trans-Golgi sacs were observed in infected cells within the first hour of infection. Extracellular virus particles were present in 5% and 30% of the cell populations at 5 and 6 h postinoculation, respectively (35). This would also facilitate the analysis, since a lower number of altered genes were involved. In the comparative transcriptomic study, far more genes (n = 136) were upregulated by SARS-CoV than by HCoV-229E. In contrast to the reported findings of increased antiapoptoptic/inflammatory gene expression and decreased proapoptotic/inflammatory gene expression in enterocyte cell lines (10), far more proapoptotic and proinflammatory genes were expressed in Huh7 cells infected by SARS-CoV but not HCoV-229E. For instance, expression of BCL2 was induced by SARS-CoV in enterocytes, yet we observed upregulation of its antagonists, including BAX and BCL2L11, in Huh7 cells. Moreover, much higher expression of other proapoptotic proteins, including CASP7, CARD10, PMAIP1, and GADD45B, was also induced by SARS-CoV than by HCoV-229E. Furthermore, there was marked perturbation of genes involved in cell cycle regulation, including induction of the CDKN2B, gene which can mediate growth arrest at the G_1 phase. The induction of proinflamma-

Downloaded from http://jvi.asm.org/ on March 10, 2015 by guest

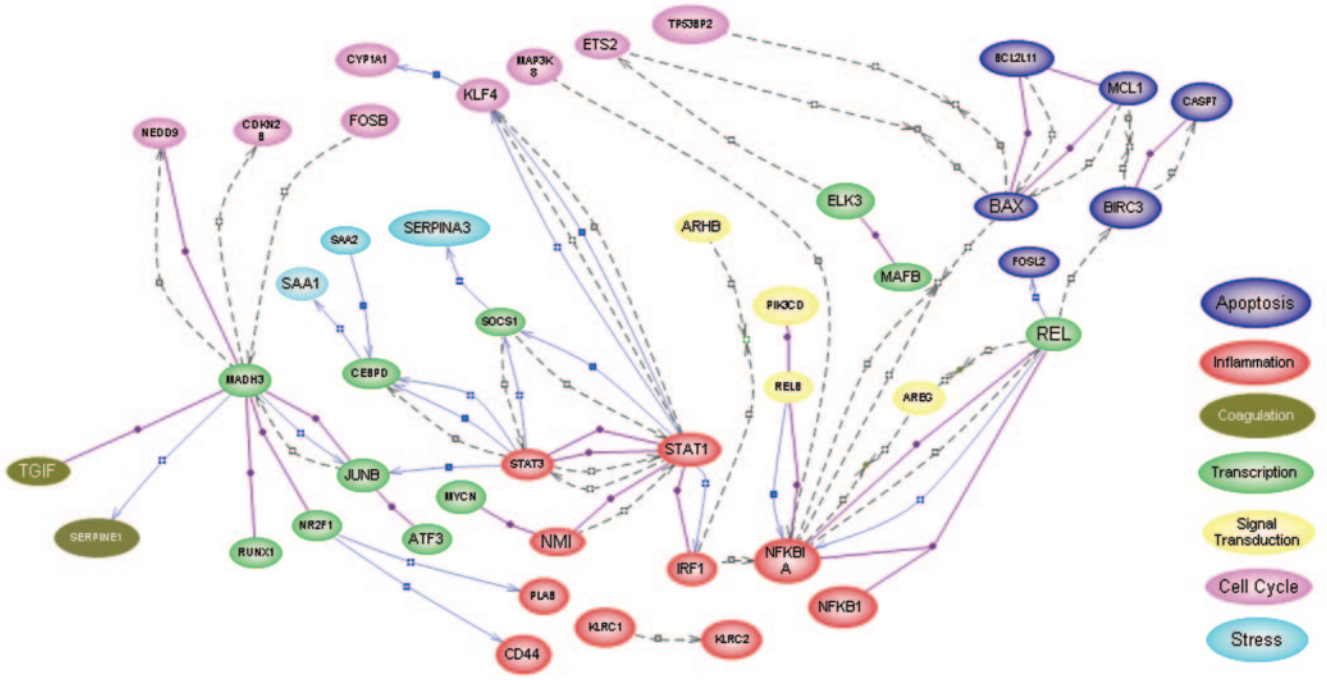

FIG. 1. Linkage of the altered genes by using Pathway Assist (version 2.53) shows clustering of genes related to apoptosis, inflammation, and coagulation. Only genes with known direct interactions are shown. The software is available from Ariadne Genomics Inc. +, upregulated/increased expression; −, downregulated/decreased expression.

tory cytokines by SARS-CoV was even more prominent when compared to HCoV-229E. The induction of IL-8 may be of pathogenic importance, as its level has been positively correlated with disease severity in pulmonary infection by respiratory syncytial virus. Thus, the observed significantly higher level of IL-8 induced by SARS-CoV compared with HCoV-229E in Huh7 cells may recapitulate the host response to these viruses by pneumocytes. The induction of various chemokines of the CXC or CCL family may mediate the chemotaxis of lymphocytes and neutrophils. These alterations in gene expression are in keeping with the histological changes of SARS hepatitis, in which cellular apoptosis, marked accumulation of cells in mitosis with ballooning degeneration of hepatocytes, and moderate lymphocytic infiltration were found in liver tissue biopsy samples (4). Recently, a vaccine study in ferrets immunized with the modified vaccinia virus Ankara carrying the spike protein showed that the ferrets developed hepatitis after being challenged with wild SARS-CoV. This finding tends to suggest that the Huh7 cell line model may have some relevance to the pathogenesis of SARS (50), but our present findings still may not be directly applicable to the pneumocytes involved in SARS.

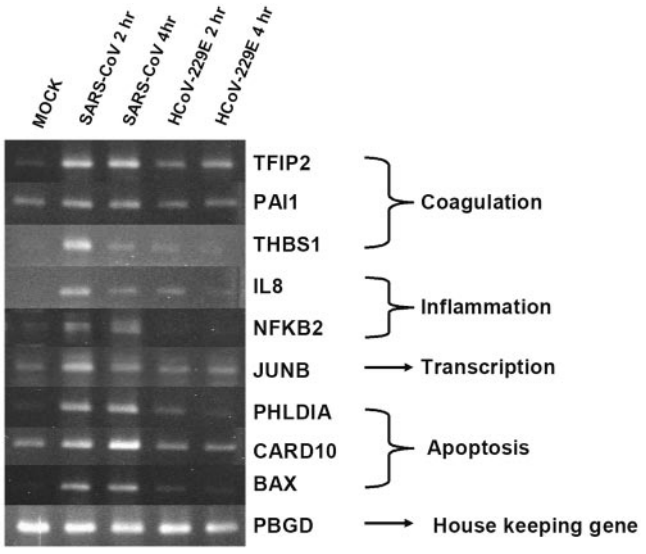

FIG. 2. Validation of microarray data by semiquantitative RT-PCR. The expression patterns of all nine selected genes and the housekeeping gene, which were assessed for their relative abundances in mock infection, at 2 h and 4 h after SARS-CoV inoculation, and at 2 h and 4 h after HCoV-229E inoculation, were consistent with the expression pattern shown in the microarray experiment.

The upregulation of genes involved in procoagulation and platelet activation was interesting. TFPI2 inhibits thrombin generation by binding and inactivation of the tissue factor-factor VIIa complex. Upregulation of the gene probably represents an inhibitory response to restrain the activation of the coagulation pathway during acute inflammation. In contrast, TFPI2 also inhibits both free and matrix/cell-associated plasmin, thus favoring fibrin deposition, and may have positive role in matrix turnover (11). Upregulation of the PAI1 gene accompanied by a dramatic increase in the protein level results in an antifibrinolytic response, favoring fibrin deposition during the acute inflammatory phase of the disease. It is important to remember that mouse hepatitis virus can activate the immune coagulation system by the fgl2 gene, encoding a prothrombi-

Downloaded from http://jvi.asm.org/ on March 10, 2015 by guest

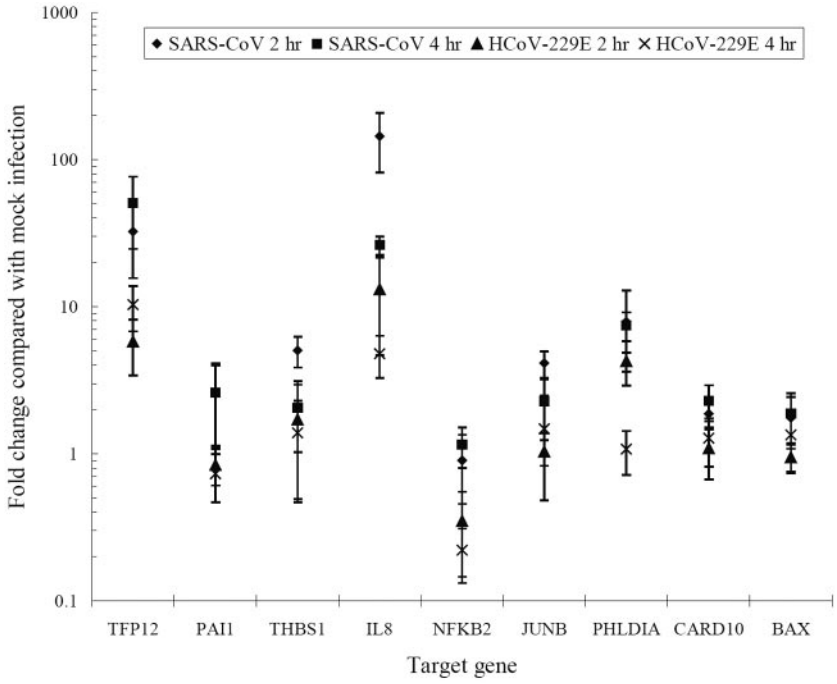

FIG. 3. Fold changes of expression of nine selected genes by RT-qPCR. The *P* values of the differences in fold changes of the target gene expressions are as follows: TFPI2 (SARS-CoV at 2 h versus HCoV-229E at 2 h), 0.02; TFPI2 (SARS-CoV at 4 h versus HCoV-229E at 4 h), 0.02; PAI1 (SARS-CoV at 2 h versus HCoV-229E at 2 h), 0.05; PAI1 (SARS-CoV at 4 h versus HCoV-229E at 4 h), 0.05; THBS1 (SARS-CoV at 2 h versus HCoV-229E at 2 h), 0.03; THBS1 (SARS-CoV at 4 h versus HCoV-229E at 4 h), 0.35; IL-8 (SARS-CoV at 2 h versus HCoV-229E at 2 h), <0.01; IL-8 (SARS-CoV at 4 h versus HCoV-229E at 4 h), <0.01; NFKB2 (SARS-CoV at 2 h versus HCoV-229E at 2 h), 0.05; NFKB2 (SARS-CoV at 4 h versus HCoV-229E at 4 h), <0.01; JUNB (SARS-CoV at 2 h versus HCoV-229E at 2 h), <0.01; JUNB (SARS-CoV at 4 h versus HCoV-229E at 4 h), 0.28; PHLDIA (SARS-CoV at 2 h versus HCoV-229E at 2 h), 0.20; PHLDIA (SARS-CoV at 4 h versus HCoV-229E at 4 h), <0.01; CARD10 (SARS-CoV at 2 h versus HCoV-229E at 2 h), 0.03; CARD10 (SARS-CoV at 4 h versus HCoV-229E at 4 h), 0.04; BAX (SARS-CoV at 2 h versus HCoV-229E at 2 h), 0.04; BAX (SARS-CoV at 4 h versus HCoV-229E at 4 h), 0.24.

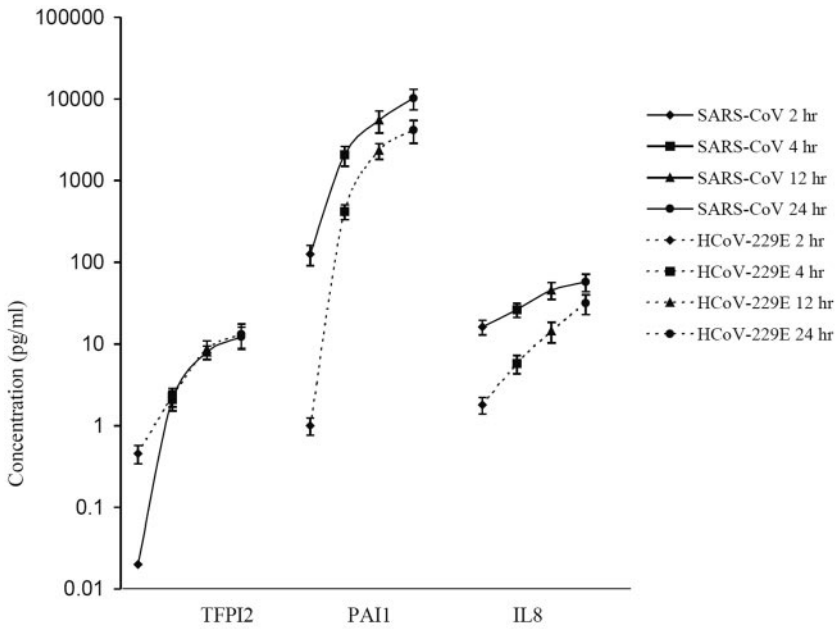

FIG. 4. Validation of protein expression for TFP1, PAI1, and IL-8 by enzyme immunoassay. The *P* values of the differences in protein expression are as follows: TFPI2 (SARS-CoV at 2 h versus HCoV-229E at 2 h), <0.01; TFPI2 (SARS-CoV at 4 h versus HCoV-229E at 4 h), 0.37; TFPI2 (SARS-CoV at 12 h versus HCoV-229E at 12 h), 0.18; TFPI2 (SARS-CoV at 24 h versus HCoV-229E at 24 h), 0.12; PAI1 (SARS-CoV at 2 h versus HCoV-229E at 2 h), <0.01; PAI1 (SARS-CoV at 4 h versus HCoV-229E at 4 h), <0.01; PAI1 (SARS-CoV at 12 h versus HCoV-229E at 12 h), <0.01; PAI1 (SARS-CoV 24 at h versus HCoV-229E at 24 h), 0.01; IL-8 (SARS-CoV at 2 h versus HCoV-229E at 2 h), <0.01; IL-8 (SARS-CoV at 4 h versus HCoV-229E at 4 h), <0.01; IL-8 (SARS-CoV at 12 h versus HCoV-229E at 12 h), <0.01; IL-8 (SARS-CoV at 24 h versus HCoV-229E at 24 h), <0.01).

Downloaded from http://jvi.asm.org/ on March 10, 2015 by guest

nase (12). This enzyme can induce macrophage procoagulation activity which results in fibrin deposition on the endothelia of intrahepatic veins and hepatic sinusoids. The end result could be confluent hepatocellular necrosis. The low number of liver biopsies done with these patients may account for the lack of reports on these full-blown changes related to vascular damage. However, systemic vasculitis, including edema, localized fibrinoid necrosis, and infiltration by monocytes, lymphocytes, and plasma cells into vessel walls in various tissues, was reported (13). Thrombosis was found in small veins. Interestingly, marked upregulation of a proapoptotic gene, PHLDA1, was observed in SARS-CoV infection of Huh7. A previous study has shown that overexpression of this gene in vascular endothelial cells would lead to decreased cell adhesion and induce detachment-mediated apoptosis. This gene, if similarly induced in vascular endothelial cells infected by SARS-CoV, may contribute to the vascular damage induced by SARS-CoV infection (21).

The clinical manifestations and histological changes involving the pneumocytes, enterocytes, and vascular endothelium were not surprising because ACE2, the host cell receptor for viral entry, was present in all these cell types (19). Similarly, abnormal urinalysis associated with increased viral load in urine is expected, since SARS-CoV could be cultured from or antigen expression could be detected in kidney cell lines and kidney tissues of patients (22). However, neither ACE2 nor L-SIGN could be detected by immunohistochemical staining in normal human hepatocytes or Huh7 (1, 42). This could be explained by an alternative cellular receptor for viral entry or just because the amount of receptor required for cell entry is so low that the cells may appear negative on immunohistochemical staining. Our previous study has shown that a high viral load in serum or stool is associated with hepatic dysfunction (22). The viral load in serum reflects the dynamic of the viral replication from any organs and the clearance mechanism of the host, whereas a high viral load in the stool may indirectly reflect the degree of portal venous viremia. Thus, the lack of cell death and inflammation in the intestine may still have importance in the pathogenesis of SARS in other body sites.

In conclusion, SARS-CoV produces more severe disturbance of host cell gene expression in a human epithelial cell line of liver origin than does HCoV-229E at the early stage of infection. There are marked alterations in gene expression related to apoptosis, inflammation, and procoagulation. These findings are consistent with the histological changes of SARS, especially in the liver and blood vessels. Besides antivirals (6, 24), other modalities of treatment, such as antiapoptotic agents (34), immunomodulators against inflammation (7), and modifiers of coagulation, should be considered in future research. It is important to remember that many patients continued to deteriorate despite a decreasing viral load 2 to 3 weeks after the onset of SARS.

ACKNOWLEDGMENTS

We thank William Mak, Carol Chan, and Tommy Tang, Genome Research Centre, The University of Hong Kong, for their excellent technical assistance. Special thanks to all the staff members of the University and Hospital Departments of Microbiology at Queen Mary Hospital.

We acknowledge research funding from the Research Fund for the Control of Infectious Diseases of the Health, Welfare and Food Bureau of the Hong Kong SAR government, Infectious Diseases Fund (William Benter), Infectious Diseases Fund (Teresa Lim), and Tung Wah Group of Hospitals Hospitals' Fund for Research in Infectious Diseases.

REFERENCES

1. **Bashirova, A. A., T. B. Geijtenbeek, G. C. van Duijnhoven, S. J. van Vliet, J. B. Eilering, M. P. Martin, L. Wu, T. D. Martin, N. Viebig, P. A. Knolle, V. N. KewalRamani, Y. van Kooyk, and M. Carrington.** 2001. A dendritic cell-specific intercellular adhesion molecule 3-grabbing nonintegrin (DC-SIGN)-related protein is highly expressed on human liver sinusoidal endothelial cells and promotes HIV-1 infection. J. Exp. Med. **193:**671–678.
2. **Chan, K. H., L. L. Poon, V. C. Cheng, Y. Guan, I. F. Hung, J. Kong, L. Y. Yam, W. H. Seto, K. Y. Yuen, and J. S. Peiris.** 2004. Detection of SARS coronavirus in patients with suspected SARS. Emerg. Infect. Dis. **10:**294–299.
3. **Chan, P. K., K. F. To, A. W. Lo, J. L. Cheung, I. Chu, F. W. Au, J. H. Tong, J. S. Tam, J. J. Sung, and H. K. Ng.** 2004. Persistent infection of SARS coronavirus in colonic cells in vitro. J. Med. Virol. **74:**1–7.
4. **Chau, T. N., K. C. Lee, H. Yao, T. Y. Tsang, T. C. Chow, Y. C. Yeung, K. W. Choi, Y. K. Tso, T. Lau, S. T. Lai, and C. L. Lai.** 2004. SARS-associated viral hepatitis caused by a novel coronavirus: report of three cases. Hepatology **39:**302–310.
5. **Che, X. Y., L. W. Qiu, Y. X. Pan, K. Wen, W. Hao, L. Y. Zhang, Y. D. Wang, Z. Y. Liao, X. Hua, V. C. Cheng, and K. Y. Yuen.** 2004. Sensitive and specific monoclonal antibody-based capture enzyme immunoassay for detection of nucleocapsid antigen in sera from patients with severe acute respiratory syndrome. J. Clin. Microbiol. **42:**2629–2635.
6. **Chen, F., K. H. Chan, Y. Jiang, R. Y. Kao, H. T. Lu, K. W. Fan, V. C. Cheng, W. H. Tsui, I. F. Hung, T. S. Lee, Y. Guan, J. S. Peiris, and K. Y. Yuen.** 2004. In vitro susceptibility of 10 clinical isolates of SARS coronavirus to selected antiviral compounds. J. Clin. Virol. **31:**69–75.
7. **Cheng, V. C., B. S. Tang, A. K. Wu, C. M. Chu, and K. Y. Yuen.** 2004. Medical treatment of viral pneumonia including SARS in immunocompetent adults. J. Infect. **49:**262–273.
8. **Cheng, V. C., I. F. Hung, B. S. Tang, C. M. Chu, M. M. Wong, K. H. Chan, A. K. Wu, D. M. Tse, K. S. Chan, B. J. Zheng, J. S. Peiris, J. J. Sung, and K. Y. Yuen.** 2004. Viral replication in the nasopharynx is associated with diarrhea in patients with severe acute respiratory syndrome. Clin. Infect. Dis. **38:**467–475.
9. **Chu, C. M., V. C. Cheng, I. F. Hung, M. M. Wong, K. H. Chan, K. S. Chan, R. Y. Kao, L. L. Poon, C. L. Wong, Y. Guan, J. S. Peiris, K. Y. Yuen, and the HKU/UCH SARS Study Group.** 2004. Role of lopinavir/ritonavir in the treatment of SARS: initial virological and clinical findings. Thorax **59:**252–256.
10. **Cinatl, J., Jr., G. Hoever, B. Morgenstern, W. Preiser, J. U. Vogel, W. K. Hofmann, G. Bauer, M. Michaelis, H. F. Rabenau, and H. W. Doerr.** 2004. Infection of cultured intestinal epithelial cells with severe acute respiratory syndrome coronavirus. Cell. Mol. Life Sci. **61:**2100–2112.
11. **Crawley, J. T., D. A. Goulding, V. Ferreira, N. J. Severs, and F. Lupu.** 2002. Expression and localization of tissue factor pathway inhibitor-2 in normal and atherosclerotic human vessels. Arterioscler. Thromb. Vasc. Biol. **22:**218–224.
12. **Ding, J. W., Q. Ning, M. F. Liu, A. Lai, J. Leibowitz, K. M. Peltekian, E. H. Cole, L. S. Fung, C. Holloway, P. A. Marsden, H. Yeger, M. J. Phillips, and G. A. Levy.** 1997. Fulminant hepatic failure in murine hepatitis virus strain 3 infection: tissue-specific expression of a novel fgl2 prothrombinase. J. Virol. **71:**9223–9230.
13. **Ding, Y., H. Wang, H. Shen, Z. Li, J. Geng, H. Han, J. Cai, X. Li, W. Kang, D. Weng, Y. Lu, D. Wu, L. He, and K. Yao.** 2003. The clinical pathology of severe acute respiratory syndrome (SARS): a report from China. J. Pathol. **200:**282–289.
14. **El-Sahly, H. M., R. L. Atmar, W. P. Glezen, and S. B. Greenberg.** 2000. Spectrum of clinical illness in hospitalized patients with "common cold" virus infections. Clin. Infect. Dis. **31:**96–100.
15. **Falsey, A. R., E. E. Walsh, and F. G. Hayden.** 2002. Rhinovirus and coronavirus infection-associated hospitalizations among older adults. J. Infect. Dis. **185:**1338–1341.
16. **Fouchier, R. A., T. Kuiken, M. Schutten, G. van Amerongen, G. J. van Doornum, B. G. van den Hoogen, M. Peiris, W. Lim, K. Stohr, and A. D. Osterhaus.** 2003. Aetiology: Koch's postulates fulfilled for SARS virus. Nature **423:**240.
17. **Gautier, I., J. Coppey, and C. Durieux.** 2003. Early apoptosis-related changes triggered by HSV-1 in individual neuronlike cells. Exp. Cell Res. **289:**174–183.
18. **Guan, Y., B. J. Zheng, Y. Q. He, X. L. Liu, Z. X. Zhuang, C. L. Cheung, S. W. Luo, P. H. Li, L. J. Zhang, Y. J. Guan, K. M. Butt, K. L. Wong, K. W. Chan, W. Lim, K. F. Shortridge, K. Y. Yuen, J. S. Peiris, and L. L. Poon.** 2003. Isolation and characterization of viruses related to the SARS coronavirus from animals in southern China. Science **302:**276–278.
19. **Hamming, I., W. Timens, M. L. Bulthuis, A. T. Lely, G. J. Navis, and H. van**

Downloaded from http://jvi.asm.org/ on March 10, 2015 by guest

Goor. 2004. Tissue distribution of ACE2 protein, the functional receptor for SARS coronavirus. A first step in understanding SARS pathogenesis. J. Pathol. **203:**631–637.
20. **Hofmann, H., K. Hattermann, A. Marzi, T. Gramberg, M. Geier, M. Krumbiegel, S. Kuate, K. Uberla, M. Niedrig, and S. Pohlmann.** 2004. S protein of severe acute respiratory syndrome-associated coronavirus mediates entry into hepatoma cell lines and is targeted by neutralizing antibodies in infected patients. J. Virol. **78:**6134–6142.
21. **Hossain, G. S., J. V. van Thienen, G. H. Werstuck, J. Zhou, S. K. Sood, J. G. Dickhout, A. B. de Koning, D. Tang, D. Wu, E. Falk, R. Poddar, D. W. Jacobsen, K. Zhang, R. J. Kaufman, and R. C. Austin.** 2003. TDAG51 is induced by homocysteine, promotes detachment-mediated programmed cell death, and contributes to the development of atherosclerosis in hyperhomocysteinemia. J. Biol. Chem. **278:**30317–30327.
22. **Hung, I. F., V. C. Cheng, A. K. Wu, B. S. Tang, K. H. Chan, C. M. Chu, M. M. Wong, W. T. Hui, L. L. Poon, D. M. Tse, K. S. Chan, P. C Woo, S. K. Lau, J. S. Peiris, and K. Y. Yuen.** 2004. Viral loads in clinical specimens and SARS manifestations. Emerg. Infect. Dis. **10:**1550–1557.
23. **Jeffers, S. A., S. M. Tusell, L. Gillim-Ross, E. M. Hemmila, J. E. Achenbach, G. J. Babcock, W. D. Thomas Jr., L. B. Thackray, M. D. Young, R. J. Mason, D. M. Ambrosino, D. E. Wentworth, J. C. Demartini, and K. V. Holmes.** 2004. CD209L (L-SIGN) is a receptor for severe acute respiratory syndrome coronavirus. Proc. Natl. Acad. Sci. USA **101:**15748–15753.
24. **Kao, R. Y., W. H. Tsui, T. S. Lee, J. A. Tanner, R. M. Watt, J. D. Huang, L. Hu, G. Chen, Z. Chen, L. Zhang, T. He, K. H. Chan, H. Tse, A. P. To, L. W. Ng, B. C. Wong, H. W. Tsoi, D. Yang, D. D Ho, and K. Y. Yuen.** 2004. Identification of novel small-molecule inhibitors of severe acute respiratory syndrome-associated coronavirus by chemical genetics. Chem. Biol. **11:**1293–1299.
25. **Koetters, P. J., L. Hassanieh, S. A. Stohlman, T. Gallagher, and M. M. Lai.** 1999. Mouse hepatitis virus strain JHM infects a human hepatocellular carcinoma cell line. Virology **264:**398–409.
26. **Ksiazek, T. G., D. Erdman, C. S. Goldsmith, S. R. Zaki, T. Peret, S. Emery, S. Tong, C. Urbani, J. A. Comer, W. Lim, P. E. Rollin, S. F. Dowell, A. E. Ling, C. D. Humphrey, W. J. Shieh, J. Guarner, C. D. Paddock, P. Rota, B. Fields, J. DeRisi, J. Y. Yang, N. Cox, J. M. Hughes, J. W. LeDuc, W. J. Bellini, L. J. Anderson, and the SARS Working Group.** 2003. A novel coronavirus associated with severe acute respiratory syndrome. N. Engl. J. Med. **348:**1953–1966.
27. **Kuiken, T., R. A. Fouchier, M. Schutten, G. F. Rimmelzwaan, G. van Amerongen, D. van Riel, J. D. Laman, T. de Jong, G. van Doornum, W. Lim, A. E. Ling, P. K. Chan, J. S. Tam, M. C. Zambon, R. Gopal, C. Drosten, S. van der Werf, N. Escriou, J. C. Manuguerra, K. Stohr, J. S. Peiris, and A. D. Osterhaus.** 2003. Newly discovered coronavirus as the primary cause of severe acute respiratory syndrome. Lancet **362:**263–270.
28. **Lau, S. K., P. C. Woo, B. H. Wong, T. W. Tsoi, G. K. Woo, R. W. Poon, K. H. Chan, W. I. Wei, J. S. Peiris, and K. Y. Yuen.** 2004. Detection of severe acute respiratory syndrome (SARS) coronavirus nucleocapsid protein in SARS patients by enzyme-linked immunosorbent assay. J. Clin. Microbiol. **42:**2884–2889.
29. **Leung, W. K., K. F. To, P. K. Chan, H. L. Chan, A. K. Wu, N. Lee, K. Y. Yuen, and J. J. Sung.** 2003. Enteric involvement of severe acute respiratory syndrome-associated coronavirus infection. Gastroenterology **125:**1011–1017.
30. **Li, W., M. J. Moore, N. Vasilieva, J. Sui, S. K. Wong, M. A. Berne, M. Somasundaran, J. L. Sullivan, K. Luzuriaga, T. C. Greenough, H. Choe, and M. Farzan.** 2003. Angiotensin-converting enzyme 2 is a functional receptor for the SARS coronavirus. Nature **426:**450–454.
31. **Lun, Z. R., and L. H. Qu.** 2004. Animal-to-human SARS-associated coronavirus transmission? Emerg. Infect. Dis. **10:**959.
32. **Marra, M. A., S. J. Jones, C. R. Astell, R. A. Holt, A. Brooks-Wilson, Y. S. Butterfield, J. Khattra, J. K. Asano, S. A. Barber, S. Y. Chan, A. Cloutier, S. M. Coughlin, D. Freeman, N. Girn, O. L. Griffith, S. R. Leach, M. Mayo, H. McDonald, S. B. Montgomery, P. K. Pandoh, A. S. Petrescu, A. G. Robertson, J. E. Schein, A. Siddiqui, D. E. Smailus, J. M. Stott, G. S. Yang, F. Plummer, A. Andonov, H. Artsob, N. Bastien, K. Bernard, T. F. Booth, D. Bowness, M. Czub, M. Drebot, L. Fernando, R. Flick, M. Garbutt, M. Gray, A. Grolla, S. Jones, H. Feldmann, A. Meyers, A. Kabani, Y. Li, S. Normand, U. Stroher, G. A. Tipples, S. Tyler, R. Vogrig, D. Ward, B. Watson, R. C. Brunham, M. Krajden, M. Petric, D. M. Skowronski, C. Upton, and R. L. Roper.** 2003. The genome sequence of the SARS-associated coronavirus. Science **300:**1399–1404.
33. **Martina, B. E., B. L. Haagmans, T. Kuiken, R. A. Fouchier, G. F. Rimmelzwaan, G. van Amerongen, J. S. Peiris, W. Lim, and A. D. Osterhaus.** 2003. SARS virus infection of cats and ferrets. Nature **425:**915.
34. **Miyamoto, D., Y. Kusagaya, N. Endo, A. Sometani, S. Takeo, T. Suzuki, Y. Arima, K. Nakajima, and Y. Suzuki.** 1998. Thujaplicin-copper chelates inhibit replication of human influenza viruses. Antiviral Res. **39:**89–100.
35. **Ng, M. L., S. H. Tan, E. E. See, E. E. Ooi, and A. E. Ling.** 2003. Proliferative growth of SARS coronavirus in Vero E6 cells. J. Gen. Virol. **84:**3291–3303.
36. **Nicholls, J. M., L. L. Poon, K. C. Lee, W. F. Ng, S. T. Lai, C. Y. Leung, C. M. Chu, P. K. Hui, K. L. Mak, W. Lim, K. W. Yan, K. H. Chan, N. C. Tsang, Y. Guan, K. Y. Yuen, and J. S. Peiris.** 2003. Lung pathology of fatal severe acute respiratory syndrome. Lancet **361:**1773–1778.
37. **Peiris, J. S., C. M. Chu, V. C. Cheng, K. S. Chan, I. F. Hung, L. L. Poon, K. I. Law, B. S. Tang, T. Y. Hon, C. S. Chan, K. H. Chan, J. S. Ng, B. J. Zheng, W. L. Ng, R. W. Lai, Y. Guan, and K. Y. Yuen, and the HKU/UCH SARS Study Group.** 2003. Clinical progression and viral load in a community outbreak of coronavirus-associated SARS pneumonia: a prospective study. Lancet **361:**1767–1772.
38. **Peiris, J. S., K. Y. Yuen, A. D. Osterhaus, and K. Stohr.** 2003. The severe acute respiratory syndrome. N. Engl. J. Med. **349:**2431–2441.
39. **Peiris, J. S., S. T. Lai, L. L. Poon, Y. Guan, L. Y. Yam, W. Lim, J. Nicholls, W. K. Yee, W. W. Yan, M. T. Cheung, V. C. Cheng, K. H. Chan, D. N. Tsang, R. W. Yung, T. K. Ng, and K. Y. Yuen, and the SARS study group.** 2003. Coronavirus as a possible cause of severe acute respiratory syndrome. Lancet **361:**1319–1325.
40. **Pene, F., A. Merlat, A. Vabret, F. Rozenberg, A. Buzyn, F. Dreyfus, A. Cariou, F. Freymuth, and P. Lebon.** 2003. Coronavirus 229E-related pneumonia in immunocompromised patients. Clin. Infect. Dis. **37:**929–932.
41. **Poggioli, G. J., R. L. DeBiasi, R. Bickel, R. Jotte, A. Spalding, G. L. Johnson, and K. L. Tyler.** 2002. Reovirus-induced alterations in gene expression related to cell cycle regulation. J. Virol. **76:**2585–2594.
42. **Pohlmann, S., E. J. Soilleux, F. Baribaud, G. J. Leslie, L. S. Morris, J. Trowsdale, B. Lee, N. Coleman, and R. W. Doms.** 2001. DC-SIGNR, a DC-SIGN homologue expressed in endothelial cells, binds to human and simian immunodeficiency viruses and activates infection in trans. Proc. Natl. Acad. Sci. USA **98:**2670–2675.
43. **Poon, L. L., O. K. Wong, K. H. Chan, W. Luk, K. Y. Yuen, J. S. Peiris, and Y. Guan.** 2003. Rapid diagnosis of a coronavirus associated with severe acute respiratory syndrome (SARS). Clin. Chem. **49:**953–955.
44. **Seto, W. H., D. Tsang, R. W. Yung, T. Y. Ching, T. K. Ng, M. Ho, L. M. Ho, and J. S. Peiris, and Advisors of the Expert SARS Group of Hospital Authority.** 2003. Effectiveness of precautions against droplets and contact in prevention of nosocomial transmission of severe acute respiratory syndrome (SARS). Lancet **361:**1519–1520.
45. **Simmons, G., J. D. Reeves, A. J. Rennekamp, S. M. Amberg, A. J. Piefer, and P. Bates.** 2004. Characterization of severe acute respiratory syndrome-associated coronavirus (SARS-CoV) spike glycoprotein-mediated viral entry. Proc. Natl. Acad. Sci. USA **101:**4240–4245.
46. **So, L. K., A. C. Lau, L. Y. Yam, T. M. Cheung, E. Poon, R. W. Yung, and K. Y. Yuen.** 2003. Development of a standard treatment protocol for severe acute respiratory syndrome. Lancet **361:**1615–1617.
47. **Vabret, A., T. Mourez, S. Gouarin, J. Petitjean, and F. Freymuth.** 2003. An outbreak of coronavirus OC43 respiratory infection in Normandy, France. Clin. Infect. Dis. **36:**985–989.
48. **van der Hoek, L., K. Pyrc, M. F. Jebbink, W. Vermeulen-Oost, R. J. Berkhout, K. C. Wolthers, P. M. Wertheim-van Dillen, J. Kaandorp, J. Spaargaren, and B. Berkhout.** 2004. Identification of a new human coronavirus. Nat. Med. **10:**368–373.
49. **van Elden, L. J., A. M. van Loon, F. van Alphen, K. A. Hendriksen, A. I. Hoepelman, M. G. van Kraaij, J. J Oosterheert, P. Schipper, R. Schuurman, and M. Nijhuis.** 2004. Frequent detection of human coronaviruses in clinical specimens from patients with respiratory tract infection by use of a novel real-time reverse-transcriptase polymerase chain reaction. J. Infect. Dis. **189:**652–657.
50. **Weingartl, H., M. Czub, S. Czub, J. Neufeld, P. Marszal, J. Gren, G. Smith, S. Jones, R. Proulx, Y. Deschambault, E. Grudeski, A. Andonov, R. He, Y. Li, J. Copps, A. Grolla, D. Dick, J. Berry, S. Ganske, L. Manning, and J. Cao.** 2004. Immunization with modified vaccinia virus Ankara-based recombinant vaccine against severe acute respiratory syndrome is associated with enhanced hepatitis in ferrets. J. Virol. **78:**12672–12676.
51. **Wong, R. S., A. Wu, K. F. To, N. Lee, C. W. Lam, C. K. Wong, P. K. Chan, M. H. Ng, L. M. Yu, D. S. Hui, J. S. Tam, G. Cheng, and J. J. Sung.** 2003. Haematological manifestations in patients with severe acute respiratory syndrome: retrospective analysis. Br. Med. J. **326:**1358–1362.
52. **Woo, P. C., S. K. Lau, B. H. Wong, H. W. Tsoi, A. M. Fung, K. H. Chan, V. K. Tam, J. S. Peiris, and K. Y. Yuen.** 2004. Detection of specific antibodies to severe acute respiratory syndrome (SARS) coronavirus nucleocapsid protein for serodiagnosis of SARS coronavirus pneumonia. J. Clin. Microbiol. **42:**2306–2309.
53. **Woo, P. C., S. K. Lau, H. W. Tsoi, K. H. Chan, B. H. Wong, X. Y. Che, V. K. Tam, S. C. Tam, V. C. Cheng, I. F. Hung, S. S. Wong, B. J. Zheng, Y. Guan, and K. Y. Yuen.** 2004. Relative rates of non-pneumonic SARS coronavirus infection and SARS coronavirus pneumonia. Lancet **363:**841–845.
54. **Yam, W. C., K. H. Chan, L. L. Poon, Y. Guan, K. Y. Yuen, W. H. Seto, and J. S. Peiris.** 2003. Evaluation of reverse transcription-PCR assays for rapid diagnosis of severe acute respiratory syndrome associated with a novel coronavirus. J. Clin. Microbiol. **41:**4521–4524.
55. **Yang, Z. Y., W. P. Kong, Y. Huang, A. Roberts, B. R. Murphy, K. Subbarao, and G. J. Nabel.** 2004. A DNA vaccine induces SARS coronavirus neutralization and protective immunity in mice. Nature **428:**561–564.
56. **Yuen, S. T., T. L. Chan, J. W. Ho, A. S. Chan, L. P. Chung, P. W. Lam, C. W. Tse, A. H. Wyllie, and S. Y. Leung.** 2002. Germline, somatic and epigenetic events underlying mismatch repair deficiency in colorectal and HNPCC-related cancers. Oncogene **21:**7585–7592.

Downloaded from http://jvi.asm.org/ on March 10, 2015 by guest